nature geoscience

Article

https://doi.org/10.1038/s41561-024-01494-2

Highly variable deep-sea currents over tidal and seasonal timescales

Received: 15 May 2023

Accepted: 27 June 2024

Published online: 25 July 2024

Check for updates

Lewis P. Bailey[1,2,3] ✉, Michael A. Clare[1], James E. Hunt[1], Ian A. Kane[4], Elda Miramontes[5,6], Marco Fonnesu[7], Ricardo Argiolas[7], Giuseppe Malgesini[8] & Regis Wallerand[9]

Deep-sea transport of sediment and associated matter, such as organic carbon, nutrients and pollutants, is controlled by near-bed currents. On the continental slope, these currents include episodic down-slope gravity-driven turbidity currents and more sustained thermohaline-driven along-slope contour currents. Recent advancements in deep-sea monitoring have catalysed a step change in our understanding of turbidity currents and contour currents individually. However, these processes rarely operate in isolation and the near-bed current regime is still to be quantified in a mixed system. Such measurements are crucial for understanding deep-sea particulate transport, calibrating numerical models and reconstructing palaeoflow. Here we use 4 years of observations from 34 instrument moorings in a mixed system offshore of Mozambique to show that near-bed currents are highly dynamic. We observe spatial variability in velocity over tidal and seasonal timescales, including reversals in current direction, and a strong steering and funnelling influence by local seabed morphology. The observed near-bed currents are capable of mobilizing and distributing sediments across the seabed, therefore complicating deep-sea particulate transport and reconstruction of palaeoceanographic conditions.

The seafloor is the ultimate sink for sediment, organic carbon and pollutants, with deposits forming an important archive of past climate, oceanography and natural hazards[1–4]. The sedimentary record, particularly on the continental slope, is dominated by the transport of material through (1) episodic down-slope gravity-driven sediment flows, termed 'turbidity currents'[5], and (2) more sustained along-slope thermohaline-driven contour currents, known as 'bottom currents'[6–9]. It is increasingly recognized that these processes rarely operate in isolation, and mixed turbidite–contourite systems, where down- and along-slope systems interact, may be the norm[10]. These interactions are most pronounced where along-slope contour currents orthogonally intersect down-slope oriented submarine canyons or channels, either directly deflecting sediment suspended by gravity flows or reshaping the morphology of their deposits[10–21]. These dynamic interactions can modify sediment transport regimes, controlling the distribution and fate of sediments, organic carbon, nutrients and pollutants[16,22–24].

Inferences about these flow interactions have previously been based on depositional records, such as the resultant channel–levee geometries and internal stratigraphic architectures, which often serve as the basis for palaeoceanographic reconstructions[19]. However, such reconstructions can be equivocal, with competing models arising from apparently similar geometries and architecture[8,13–15,25]. Uncertainty primarily stems from a paucity of direct monitoring of the near-bed current regime in mixed depositional systems[26]. Recent advances

[1]National Oceanography Centre, Southampton, UK. [2]School of Ocean and Earth Science, University of Southampton, Southampton, UK. [3]Department of Earth, Energy and Environment, University of Calgary, Calgary, Alberta, Canada. [4]School of Earth and Environmental Sciences, University of Manchester, Manchester, UK. [5]Faculty of Geosciences, University of Bremen, Bremen, Germany. [6]MARUM–Center for Marine Environmental Sciences, University of Bremen, Bremen, Germany. [7]Eni Upstream and Technical Services, Milano, Italy. [8]RINA Consulting, Milano, Italy. [9]TotalEnergies, Paris, France. ✉e-mail: Lewis.Bailey@UCalgary.ca

https://doi.org/10.1038/s41561-024-01494-2

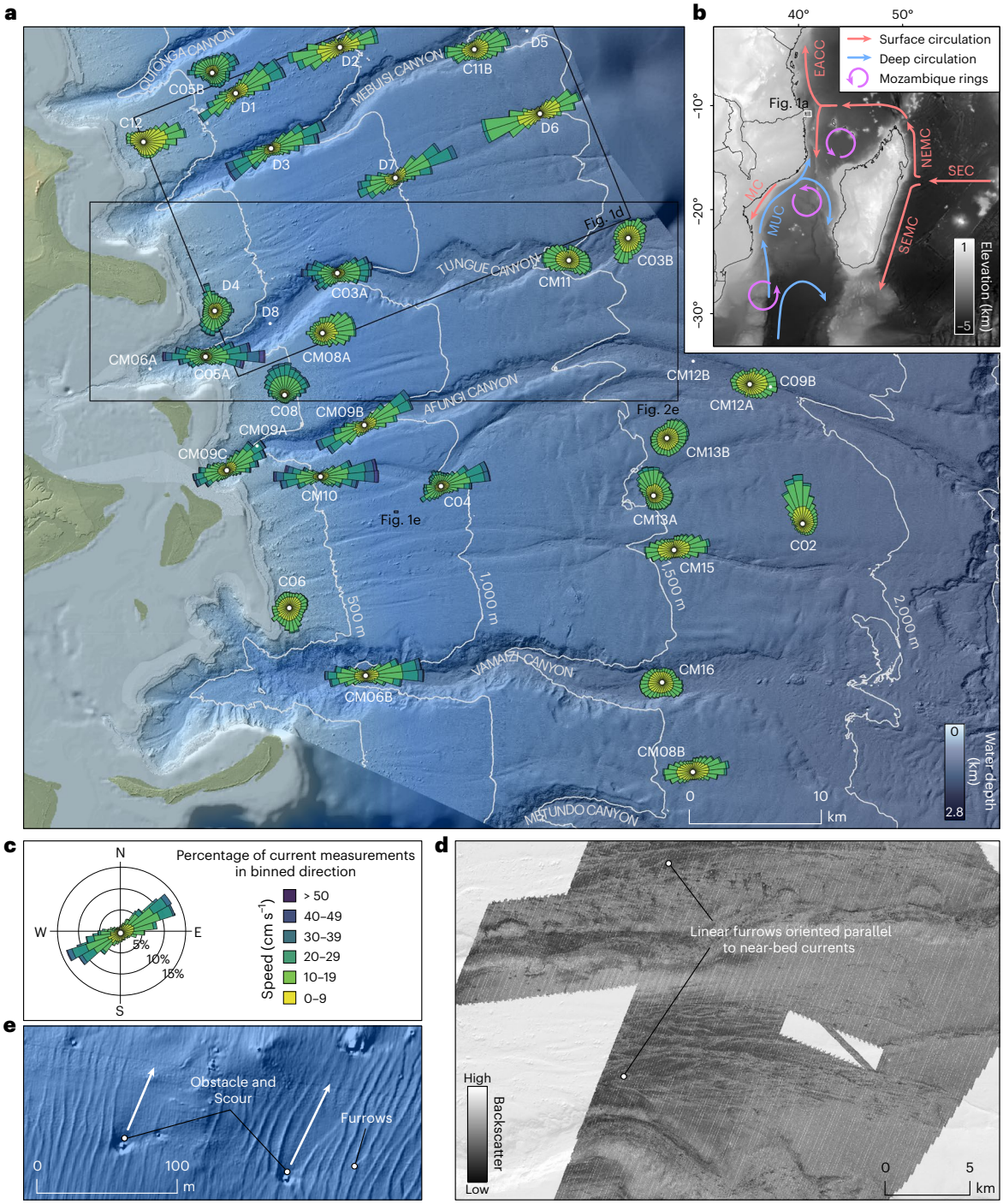

Fig. 1 | Observations of near-bed currents offshore North Mozambique. **a**, Rose diagrams showing current direction as a percentage of total measurements from closest to seabed bin at each mooring (Supplementary Table 1). The arm colour divisions refers to abundance of recorded velocities as shown in **c**. **b**, Bathymetry (GEBCO, 2022) offshore East Africa showing location of study site and regional ocean circulation patterns. SEC, South Equatorial Current; SEMC, Southeast Madagascar Current. **c**, The legend for rose diagrams in **a**. **d**, E–W trending linear furrows from multi-beam backscatter (5 m bin size) oriented parallel to seafloor currents proximal to gullies most probably reflect changes in grain size. **e**, Furrows and scours at the seabed (0.6 m bin size, remotely operated vehicle multi-beam) indicate the dominance of north-flowing bottom currents.

in deep-sea monitoring, particularly the long-term deployment of acoustic Doppler current profilers (ADCPs), have catalysed a step change in our understanding of turbidity currents[5] and demonstrated the seasonality of contour currents[9]. Fewer equivalent measurements exist in mixed systems. Such monitoring campaigns have suggested that currents are steered by seabed relief[27,28]. However, these measurements do not truly characterize the near-bed regime as observations were generally recorded far above the seabed (tens of metres to 100 m). Understanding near-bed current variability over different space and timescales is critical for our knowledge of sediment (and associated particulate matter) re-suspension and transport, especially in mixed systems where gravity flow–contour current interactions can fundamentally modify transport pathways[15,25].

To progress our understanding of deep-sea particulate transport, calibrate numerical models and enable robust palaeoflow reconstructions, there is a compelling need to acquire field-scale current

https://doi.org/10.1038/s41561-024-01494-2

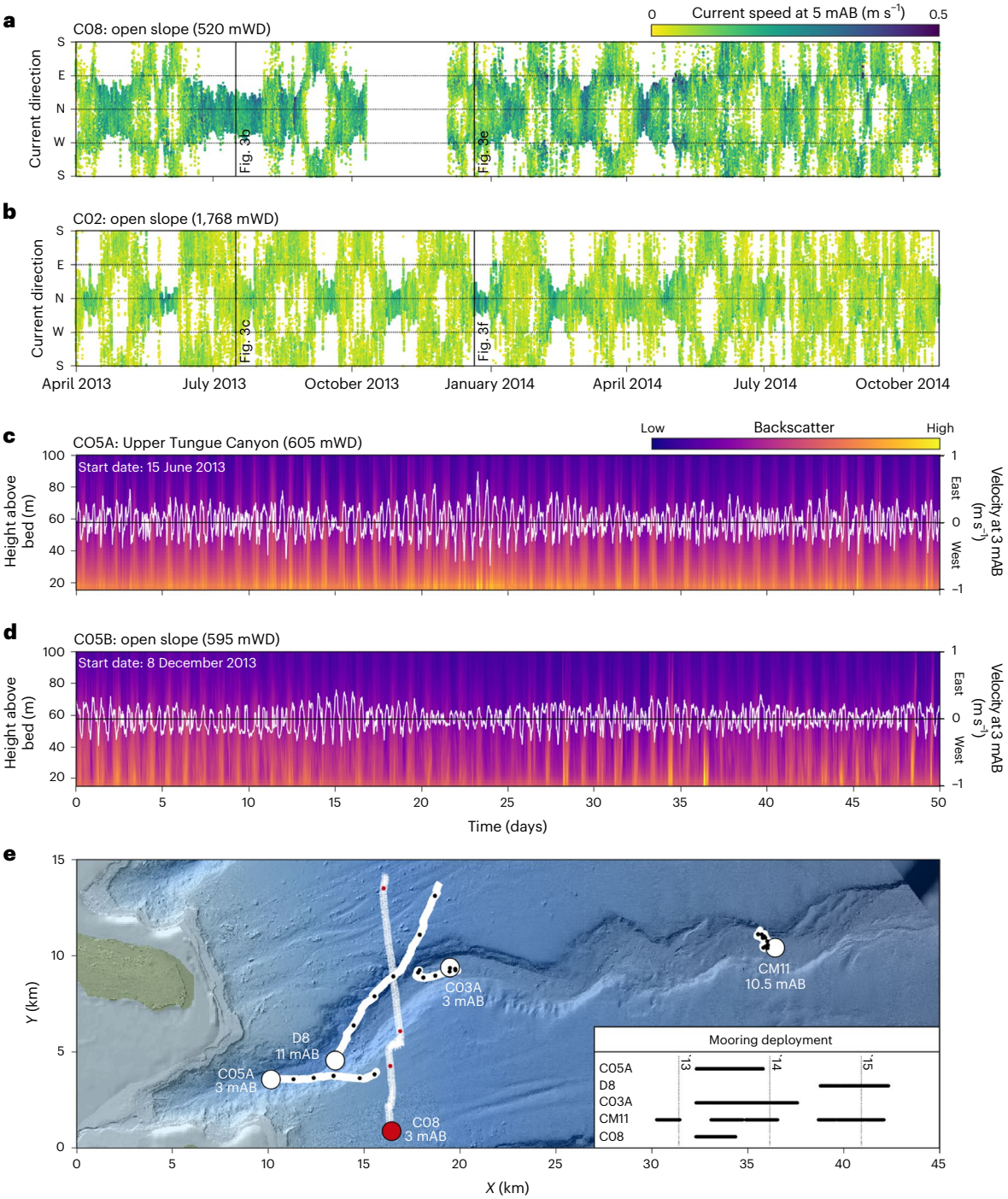

Fig. 2 | Time series showing the spatial and temporal variation in near-bed current velocity. a,**b**, Open slope velocity 3 mAB at C08 (**a**) and CO2 (**b**). Black vertical lines indicate the time of modelled currents in Fig. 3. **c**,**d**, Current measurements at 3 mAB coupled with ADCP acoustic backscatter between 15 and 100 mAB within the upper section of Tungue Canyon at C05A (**c**) and on the open slope at C05B (**d**). Note that the 50 day intervals of **c** and **d** do not correspond. **e**, Cumulative vector plots of near-bed currents at mooring locations within Tungue Canyon (C05A, D8, C03A and CM11) and the open slope (C08). Data are from closest bin to seabed (Supplementary Table 1). Black and red data points represent 50 day intervals. The insert shows the duration of instrument deployment and vector plots show data from all periods of monitoring. Location and water depth shown in Fig. 1a.

measurements proximal to seabed in mixed turbidite–contourite systems. Here, using a spatially- and temporally-extensive monitoring array, we integrate near-bed (to within 3 m of the seabed) current measurements (comprising both thermohaline and tidal components) made at 34 mooring locations (Fig. 1a) over a 4 year monitoring period (Supplementary Table 1), with >2,500 km^2 of high-resolution seabed multi-beam bathymetry spanning a mixed turbidite–contourite depositional system, on the Mozambique continental slope (Fig. 1). The system comprises of a series of east–west (E–W) trending submarine canyons that extend ~70 km offshore (Fig. 1a), with low modern terrestrial sediment supply[29], and is located in a region of complex and highly energetic ocean currents (Fig. 1b)[12,30–37]. Using these unprecedented synchronous and spatially- distributed measurements, we quantify the dynamic interactions across a large mixed depositional system and address the following questions. First, how does near-bed current velocity vary temporally and spatially across a large

https://doi.org/10.1038/s41561-024-01494-2

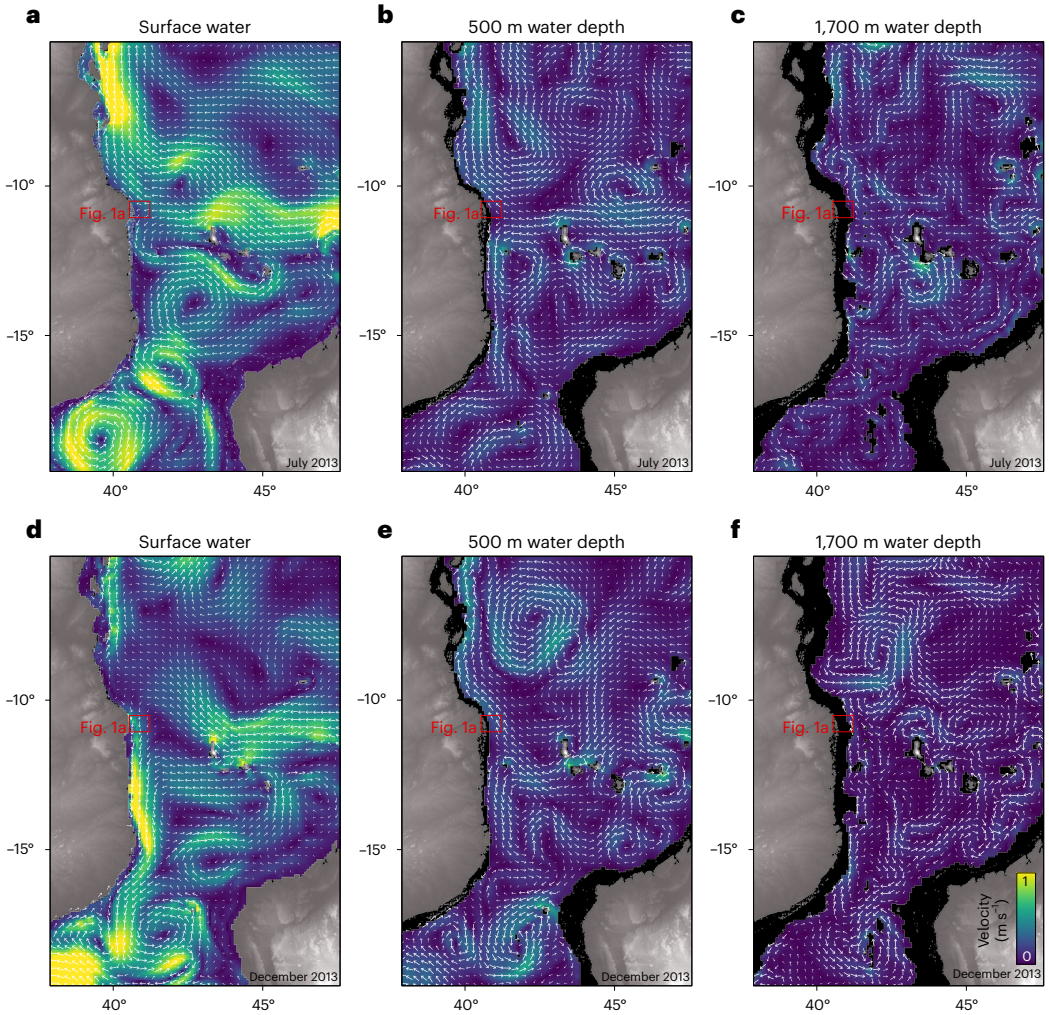

Fig. 3 | Modelled regional seawater velocity. a–c, Modelled seawater velocity when a mesoscale eddy is located to the south of the study site on 16 July 2013 at the sea surface (**a**), at 500 m (**b**) and 1,700 m water depths (**c**). **d–f**, Modelled seawater velocity when the NEMC splits to the north of the study area on 21 December 2013 at the sea surface (**d**), at 500 m (**e**) and 1,700 m water depths (**f**). Size range of vector arrows in each panel are relative to the range of velocities observed for each given date and water depth. The site of multi-beam bathymetry and moored instruments are shown by the location of Fig. 1a.

mixed system? Second, to what extent does seabed relief influence near-bed currents and over what spatial scale? Specifically, how do orthogonally-oriented currents interact with topographic features? Finally, what are the implications of the diverse interactions we observe for particulate transport and deposition in mixed systems?

Variability in regional near-bed current velocity

Direct near-bed measurements on the open-slope areas show a dominance of northward-directed near-seafloor currents, with velocities of typically 0.2–0.4 m s^{-1} and the fastest currents (up to 0.6 m s^{-1}) observed in shallower (<500 m) water depths (Figs. 1a and 2a,b). These measurements are consistent with the formation of north-to-northeast trending obstacle-scour seabed features (Fig. 1e) and asymmetric canyon and channel cross-sectional morphologies[15]. The dominant northward flow, especially in deeper (>1,500 m) water, is consistent with previous observations of the Mozambique Undercurrent[35] (MUC; Fig. 1b). While the northward extent of the MUC is not clearly defined, modelled currents show a prevalent northward current through the study site at 1,700 m water depth (for example, Fig. 3f).

Our long-duration measurements reveal that near-bed flow is not persistent, and its intensity and direction vary temporally, sometimes reversing over periods of days to weeks. A net-northward transport of near-bed water masses along the entire slope is observed[15] (C08 in Fig. 2e) due to the fastest near-bed currents coinciding with a northward flow direction (Figs. 1a and 2a,b). This transient switching of near-bed current direction could easily be missed by shorter-duration monitoring, potentially leading to misinterpretation of the net direction of the regional current. Indeed, we observe further variations on even shorter timescales, wherein the velocity of near-bed currents fluctuates across tidal cycles (Figs. 1a,b and 2d). Furthermore, the timing of the multiple subannual current reversals is not always synchronous along the slope (Fig. 2a,b). These observations underline the value of sustained near-bed current measurements at multiple locations, and demonstrates that contour currents are clearly far from steady, continuous flows, and can be extremely dynamic, varying in speed and direction across subannual timescales.

Temporal and spatial variability of measured current velocity offshore North Mozambique probably reflects the complex ocean circulation of the region[12,30–36]. The direction of surface water flow alternates depending on seasonal shifts in latitude where the Northeast Madagascar Current (NEMC) splits along the African margin[36] (that is, when the NEMC splits north of the study site surface currents trend to the south, and vice versa; Fig. 3a,d). Additionally, regional modelling of currents shows that the intensity of deeper (>500 m) northward trending currents within the study area diminishes when mesoscale eddies are present to the south (for example, lower velocity observed in July 2013

https://doi.org/10.1038/s41561-024-01494-2

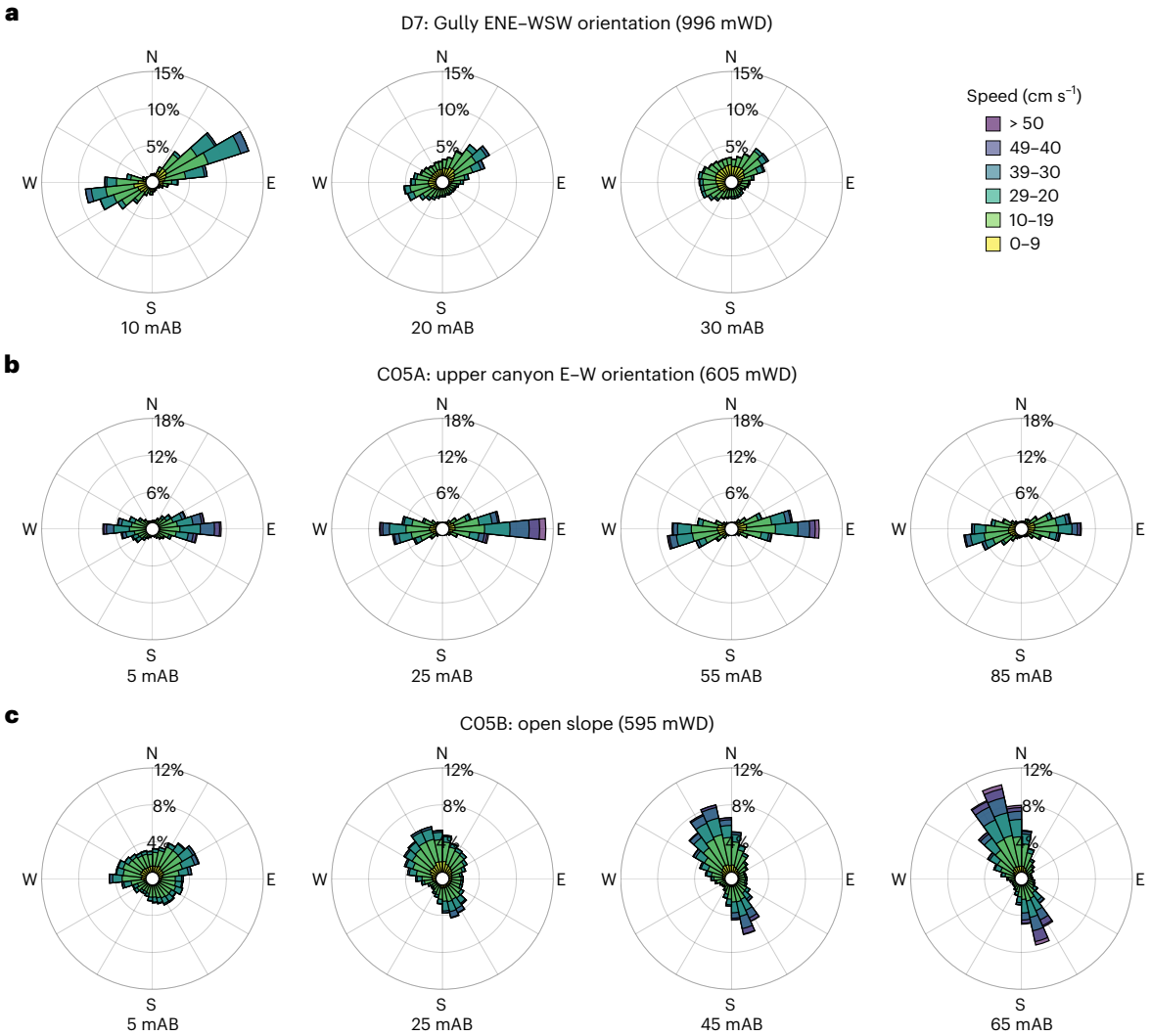

Fig. 4 | Near-bed current speed and direction rose diagrams with increasing height above the seabed. **a**, Reduced influence of topographic steering with increasing height above a gully at mooring D7. **b**, Continued confinement of currents within a submarine canyon at mooring C05A. **c**, Changes in current direction with increasing height above the seabed on the open slope at C05B. Measurements from C05A and C05B at 5 mAB are recorded by current metres, all other measurements were acquired from ADCPs. The rose diagrams show current direction as a percentage of total measurement from a given height above the seabed. The arm colour divisions refer to abundance of recorded velocities 10 cm s^{-1} intervals. ENE–WSW, east-northeast to west-southwest.

(Fig. 3b,c) compared with December 2013 (Fig. 3e,f)), consistent with observations of the MUC intensity in the Mozambique Channel[12,31].

Topographic steering of near-bed currents

Net-northward near-bed flow is not observed in all moored instruments (Fig. 1a). For example, within submarine canyons, current direction is modulated on a tidal frequency, producing a clear semi-diurnal (M_2) and tidal (M_4) signal (for example, C05A in Tungue Canyon; Extended Data Fig. 1) in an up- and down-canyon oriented flow (approximately E–W; Figs. 1a and 2c). Moored ADCPs did not record turbidity currents during the deployment period (despite the observations of crescentic bedforms, sediment waves and knickpoints providing morphological evidence of their past activity; Fig. 1a and Extended Data Fig. 2). Instead, the most intense near-bed currents are observed in the upper reaches and heads of canyons (up to 0.95 m s^{-1}; Figs. 1a and 2c and Supplementary Table 2) with current magnitude decreasing down-canyon with increasing water depth (as observed on the open slope). Perhaps more surprisingly, low relief gullies (typically 20 m deep) show similar near-bed current deflection towards their axes (for example, D7; Fig. 1a). The up-slope- and down-slope-oriented flow in topographic features can extend onto the adjacent open slope. For example, moorings C04 and C05B, positioned on open slope ~1 km outside of a canyon both record a dominant E–W current regime near bed (Fig. 1a), though not as intense and persistent as within submarine canyons. Further comparison indicates that velocity oscillations were greater at C05A (within the submarine canyon) than C05B (Fig. 2c,d). This regime contrasts with other measurements on the open slope (for example, C02, C08 and CM13A; Fig. 1a) where only a slight (that is, northeast–northwest) deflection to the prevailing north-trending current is observed. The observed spatial variation demonstrates the influence of seafloor morphology, where internal tides are captured and funnelled by the steep confining topography.

The net direction of near-bed currents can vary substantially within an individual canyon. For example, the two shallowest moorings within Tungue Canyon (C05A and D8 at 605 m and 746 m water depth, respectively) reveal a strongly net down-canyon near-bed flow, whereas net flow is up canyon in deeper canyon reaches (C03A at 1014 and CM11 at 1,583 m water depth; Fig. 2e). The net up-canyon current at the distal moorings is interpreted as an internal tidal bore which is then strongly reflected back down-canyon when it hits the steep bathymetry in canyon heads, as observed in other deep-sea submarine canyons[23,38–41]. The net direction of displacement also

varies temporally as well as spatially. For instance, measurements at C03A (1,014 m water depth in Tungue Canyon; Fig. 1a) reveal short-lived (weeks) intervals where near-bed flow is counter to the net westward-directed flow (Fig. 2e). This reversal further demonstrates the importance of sufficiently long measurement periods to capture the true net direction of flow.

The influence of topographic steering diminishes with distance from seabed. For example, axis-parallel currents are recorded at 10 m above bed (mAB) within a low relief northeast–southwest trending gully, but the topographic influence is barely recognizable at 30 mAB (Fig. 4a). The much greater topographic confinement provided by submarine canyons ensures that currents are consistently aligned with the canyon thalweg at all elevations measured by the ADCP (that is, from 5 m to 85 mAB; Fig. 4b). No measurements were made above the height of the canyon, hence it is not possible to determine at precisely what height above seabed this influence is no longer felt. However, while canyons probably fundamentally affect near-bed current steering over at least their full height (~200 m), the influence of the adjacent submarine canyon at mooring C05B (Fig. 1a) is seemingly only restricted to the bottom few metres and is indiscernible by 25 mAB (Fig. 4c). These findings again highlight the need for near-bed measurements to truly quantify near-bed flow.

Implications for sediment transport

While morphological evidence exists for down-canyon sediment transport (Fig. 1a and Extended Data Fig. 1), the absence of ADCP-recorded turbidity currents and lack of bedform migration observed from repeat seabed mapping, coupled with the low present-day sediment supply[29], suggests that the submarine canyons are currently largely inactive with respect to gravity flows[42]. However, enhanced ADCP acoustic backscatter documents the contemporary transport of suspended sediment within submarine canyons and along the adjacent slope (for example, C05A and C05B), with the highest backscatter coinciding with peaks in near-bed current velocity (Fig. 2c,d and Extended Data Fig. 1). Very high sediment concentrations (that is, >1 g l^{-1}) are unlikely given that the ADCP measurements are not fully attenuated (that is, signal penetrates to seafloor)[43,44]. However, according to near-bed measurements, current speeds can exceed the threshold to initiate motion of the sampled silt to medium sand grain sizes (critical Shields parameter is exceeded; Methods), aside from the coarsest grain fraction observed in upper submarine canyons susceptible to transport through re-suspension (Rouse number >1.2; Methods, Supplementary Table 3 and Supplementary Fig. 1). Streaked seabed accumulations of sand oriented parallel to submarine canyons and gullies (interpreted from multi-beam backscatter data[45]; Fig. 1d and Supplementary Table 3) further indicate that near-bed currents are capable of mobilizing and (re)distributing sediment across the seafloor, in a direction that is orthogonal to the regional thermohaline-driven current. Therefore, it is near-bed currents and internal tides steered by topography that are the dominant mechanism for the contemporary transport of sediment[46] (and associated matter, such as organic carbon and pollutants, which are similarly susceptible to redistribution by near-bed currents[22–24]), whereby local net-down-slope transfer is modulated at tidal frequencies (Fig. 2c,d).

While modern sediment supplies are restricted, a stock of sediment deposited by past gravity currents is available for reworking and redistribution by near-seafloor currents along canyons. The reworking influence of contour currents may not extend to the base of highly confined channels[16]. However, we show that the confining topography funnels near-bed currents, creating axis-parallel flows capable of re-suspending sediment (Figs. 1a and 2c,d and Extended Data Fig. 2). The role of topographically funnelled near-bed currents, which can exceed 1 m s^{-1} in many submarine canyons[23,38,47–50], may have been dramatically underestimated in many mixed systems. The resultant deposits which will probably comprise reworked turbidites may be indiscernible from those emplaced by gravity currents, therefore complicating the calculation of turbidity current recurrence intervals and reconstruction of palaeo-currents.

The wide variability in current velocity observed across 34 mooring locations underlines the challenges that remain in characterizing seafloor currents, even when direct measurements are available. Near-bed processes are clearly complex and sedimentation across the study area is probably controlled by the combination and interaction of different processes. Our new observations highlight the value of sustained near-bed current measurements at multiple locations in understanding deep-sea transport systems and the resultant dynamic distribution and accumulation of sediment, carbon and pollutants.

Online content

Any methods, additional references, Nature Portfolio reporting summaries, source data, extended data, supplementary information, acknowledgements, peer review information; details of author contributions and competing interests; and statements of data and code availability are available at https://doi.org/10.1038/s41561-024-01494-2.

References

1. Llave, E. et al. High-resolution stratigraphy of the Mediterranean outflow contourite system in the Gulf of Cadiz during the late Pleistocene: the impact of Heinrich events. *Mar. Geol.* **227**, 241–262 (2006).
2. Woodall, L. C. et al. The deep sea is a major sink for microplastic debris. *R. Soc. Open Sci.* **1**, 140317 (2014).
3. Legge, O. et al. Carbon on the Northwest European Shelf: contemporary budget and future influence. *Front. Mar. Sci.* **7**, 143 (2020).
4. van der Voort, T. S. et al. MOSAIC (Modern Ocean Sediment Archive and Inventory of Carbon): a (radio)carbon-centric database for seafloor surficial sediments. *Earth Syst. Sci. Data* **13**, 2135–2146 (2021).
5. Talling, P. J. et al. Detailed monitoring reveals the nature of submarine turbidity currents. *Nat. Rev. Earth Environ.* **4**, 642–658 (2023).
6. Heezen, B. C., Hollister, C. D. & Ruddiman, W. F. Shaping of the continental rise by deep geostrophic contour currents. *Science* **152**, 502–508 (1966).
7. Faugères, J.-C. & Stow, D. A. V. in *Developments in Sedimentology* Vol. 60 (eds Rebesco, M. & Camerlenghi, A.) 257–288 (Elsevier, 2008).
8. Rebesco, M., Hernández-Molina, F. J., Van Rooij, D. & Wåhlin, A. Contourites and associated sediments controlled by deep-water circulation processes: state-of-the-art and future considerations. *Mar. Geol.* **352**, 111–154 (2014).
9. Zhao, Y. et al. In situ observation of contour currents in the northern South China Sea: applications for deepwater sediment transport. *Earth Planet. Sci. Lett.* **430**, 477–485 (2015).
10. Rodrigues, S. et al. A new classification system for mixed (turbidite–contourite) depositional systems: examples, conceptual models and diagnostic criteria for modern and ancient records. *Earth Sci. Rev.* **230**, 104030 (2022).
11. Mulder, T., Faugères, J.-C. & Gonthier, E. in *Developments in Sedimentology* Vol. 60 (eds Rebesco, M. & Camerlenghi, A.) 435–456 (Elsevier, 2008).
12. Miramontes, E. et al. The influence of bottom currents on the Zambezi Valley morphology (Mozambique Channel, SW Indian Ocean): in situ current observations and hydrodynamic modelling. *Mar. Geol.* **410**, 42–55 (2019).
13. Sansom, P. Hybrid turbidite–contourite systems of the Tanzanian margin. *Pet. Geosci.* **24**, 258–276 (2018).
14. Fonnesu, M. et al. A new world-class deep-water play-type, deposited by the syndepositional interaction of turbidity flows and bottom currents: the giant Eocene coral field in northern Mozambique. *Mar. Pet. Geol.* **111**, 179–201 (2020).

15. Fuhrmann, A. et al. Hybrid turbidite–drift channel complexes: an integrated multiscale model. *Geology* **48**, 562–568 (2020).
16. Fuhrmann, A., Kane, I. A., Schomacker, E., Clare, M. A. & Pontén, A. Bottom current modification of turbidite lobe complexes. *Front. Earth Sci.* **9**, 752066 (2022).
17. Hernández-Molina, F. J., Larter, R. D. & Maldonado, A. Neogene to quaternary stratigraphic evolution of the antarctic peninsula, pacific margin offshore of adelaide island: transitions from a non-glacial, through glacially-influenced to a fully glacial state. *Glob. Planet. Change* **156**, 80–111 (2017).
18. Pandolpho, B. T. et al. Seismic record of a cyclic turbidite-contourite system in the Northern Campos Basin, SE Brazil. *Mar. Geol.* **434**, 106422 (2021).
19. Rodrigues, S., Hernández-Molina, F. J. & Kirby, A. A Late Cretaceous mixed (turbidite–contourite) system along the Argentine margin: paleoceanographic and conceptual implications. *Mar. Pet. Geol.* **123**, 104768 (2021).
20. Shanmugam, G., Spalding, T. D. & Rofheart, D. H. Process sedimentology and reservoir quality of deep-marine bottom-current reworked sands (sandy contourites): an example from the Gulf of Mexico. *AAPG Bull.* **77**, 1241–1259 (1993).
21. Thiéblemont, A., Hernández-Molina, F. J., Miramontes, E., Raisson, F. & Penven, P. Contourite depositional systems along the Mozambique channel: the interplay between bottom currents and sedimentary processes. *Deep Sea Res. I Oceanogr. Res. Pap.* **147**, 79–99 (2019).
22. Magill, C. R. et al. Transient hydrodynamic effects influence organic carbon signatures in marine sediments. *Nat. Commun.* **9**, 4690 (2018).
23. Maier, K. L. et al. Sediment and organic carbon transport and deposition driven by internal tides along Monterey Canyon, offshore California. *Deep Sea Res. I Oceanogr. Res. Pap.* **153**, 103108 (2019).
24. Kane, I. A. et al. Seafloor microplastic hotspots controlled by deep-sea circulation. *Science* **368**, 1140–1145 (2020).
25. Miramontes, E. et al. Channel-levee evolution in combined contour current–turbidity current flows from flume-tank experiments. *Geology* **48**, 353–357 (2020).
26. McCave, I. N., Thornalley, D. J. R. & Hall, I. R. Relation of sortable silt grain-size to deep-sea current speeds: calibration of the 'Mud Current Meter'. *Deep Sea Res. I Oceanogr. Res. Pap.* **127**, 1–12 (2017).
27. Steinmann, L. et al. Discovery of a giant cold-water coral mound province along the northern Argentine margin and its link to the regional contourite depositional system and oceanographic setting. *Mar. Geol.* **427**, 106223 (2020).
28. Wilckens, H. et al. The erosive power of the malvinas current: influence of bottom currents on morpho-sedimentary features along the northern Argentine margin (SW Atlantic Ocean). *Mar. Geol.* **439**, 106539 (2021).
29. Maselli, V. et al. Impact of the east african rift system on the routing of the deep-water drainage network offshore tanzania, western Indian Ocean. *Basin Res.* **32**, 789–803 (2020).
30. de Ruijter, W. P. M., Ridderinkhof, H., Lutjeharms, J. R. E., Schouten, M. W. & Veth, C. Observations of the flow in the Mozambique Channel. *Geophys. Res. Lett.* **29**, 140-1–140–3 (2002).
31. Schouten, M. W., de Ruijter, W. P. M., van Leeuwen, P. J. & Ridderinkhof, H. Eddies and variability in the Mozambique Channel. *Deep Sea Res. II Top. Stud. Oceanogr.* **50**, 1987–2003 (2003).
32. Ullgren, J. E., André, E., Gammelsrød, T. & Hoguane, A. M. Observations of strong ocean current events offshore Pemba, northern Mozambique. *J. Oper. Oceanogr.* **9**, 55–66 (2016).
33. van Aken, H. M., Ridderinkhof, H. & de Ruijter, W. P. M. North Atlantic deep water in the south-western Indian Ocean. *Deep Sea Res. I Oceanogr. Res. Pap.* **51**, 755–776 (2004).
34. Schott, F. A., Xie, S.-P. & McCreary, J. P. Jr. Indian Ocean circulation and climate variability. *Rev. Geophys.* **47**, RG1002 (2009).
35. Ullgren, J. E., van Aken, H. M., Ridderinkhof, H. & de Ruijter, W. P. M. The hydrography of the Mozambique Channel from six years of continuous temperature, salinity, and velocity observations. *Deep Sea Res. I Oceanogr. Res. Pap.* **69**, 36–50 (2012).
36. Collins, C., Hermes, J. C., Roman, R. E. & Reason, C. J. C. First dedicated hydrographic survey of the Comoros Basin. *J. Geophys. Res. Oceans* **121**, 1291–1305 (2016).
37. Collins, C., Hermes, J. C. & Reason, C. J. C. Mesoscale activity in the Comoros Basin from satellite altimetry and a high-resolution ocean circulation model. *J. Geophys. Res. Oceans* **119**, 4745–4760 (2014).
38. Petruncio, E. T., Rosenfeld, L. K. & Paduan, J. D. Observations of the internal tide in Monterey Canyon. *J. Phys. Oceanogr.* **28**, 1873–1903 (1998).
39. Zhao, Z., Alford, M. H., Lien, R.-C., Gregg, M. C. & Carter, G. S. Internal tides and mixing in a submarine canyon with time-varying stratification. *J. Phys. Oceanogr.* **42**, 2121–2142 (2012).
40. Waterhouse, A. F. et al. Internal tide convergence and mixing in a submarine canyon. *J. Phys. Oceanogr.* **47**, 303–322 (2017).
41. Hall, R. A., Aslam, T. & Huvenne, V. A. I. Partly standing internal tides in a dendritic submarine canyon observed by an ocean glider. *Deep Sea Res. I: Oceanogr. Res. Pap.* **126**, 73–84 (2017).
42. Bailey, L. P. et al. Preconditioning by sediment accumulation can produce powerful turbidity currents without major external triggers. *Earth Planet. Sci. Lett.* **562**, 116845 (2021).
43. Simmons, S. M. et al. Novel acoustic method provides first detailed measurements of sediment concentration structure within submarine turbidity currents. *J. Geophys. Res. Oceans* **125**, e2019JC015904 (2020).
44. Ha, H. K., Maa, J. P.-Y., Park, K. & Kim, Y. H. Estimation of high-resolution sediment concentration profiles in bottom boundary layer using pulse-coherent acoustic Doppler current profilers. *Mar. Geol.* **279**, 199–209 (2011).
45. Principaud, M. et al. Recent morphology and sedimentary processes along the western slope of Great Bahama Bank (Bahamas). *Sedimentology* **65**, 2088–2116 (2018).
46. Cacchione, D. A., Pratson, L. F. & Ogston, A. S. The shaping of continental slopes by internal tides. *Science* **296**, 724–727 (2002).
47. Shepard, F. P. Submarine canyons. *Earth Sci. Rev.* **8**, 1–12 (1972).
48. Aslam, T., Hall, R. A. & Dye, S. R. Internal tides in a dendritic submarine canyon. *Prog. Oceanogr.* **169**, 20–32 (2018).
49. Martín, J., Palanques, A., Vitorino, J., Oliveira, A. & de Stigter, H. C. Near-bottom particulate matter dynamics in the Nazaré submarine canyon under calm and stormy conditions. *Deep Sea Res. II Top. Stud. Oceanogr.* **58**, 2388–2400 (2011).
50. Lee, I.-H., Wang, Y.-H., Liu, J. T., Chuang, W.-S. & Xu, J. Internal tidal currents in the Gaoping (Kaoping) submarine canyon. *J. Mar. Syst.* **76**, 397–404 (2009).

Methods

Field site and setting

The study area comprises a mixed turbidite–contourite depositional system offshore of Mozambique, East Africa. The present-day Mozambique slope lies offshore from a narrow (10–20 km) mixed carbonate-siliciclastic shelf bounded on the seaward edge by a barrier island system and a steep (up to 70°) shelf break. A sequence of E–W trending submarine canyons occurs along the continental slope, cutting into the shelf break, and incising up to 200 m vertically. The morphology of individual canyons is variable, but all terminate at or before the intersection with the Davie fracture zone ~70 km offshore[51]. The Rovuma Delta (located to the north of the study area) was a major depositional environment through most of the Tertiary period[52]. However, the development of the East African Rift system during the Cenozoic strongly modified continental drainage patterns[53]. A series of ephemeral rivers discharge onto the shelf, but these do not directly connect to canyon heads, and modern sediment supply to canyon heads is low[29].

Ocean currents offshore of Mozambique are complex and can be highly energetic[30,33]. Circulation is strongly influenced by the NEMC. The NEMC diverges to the northward flowing East African Coastal Current (EACC) and the southward-bound Mozambique Current (MC)[36], which forms part of the Agulhas Current system, the strongest western boundary current in the Southern Hemisphere[54] (Fig. 1). The latitude where the NEMC splits along the African margin varies seasonally[34,36]. The deeper-water regime (>800 m water depth) is dominated by the north-flowing MUC. At the narrowest point between Mozambique and Madagascar, the MUC has been analysed at 1,500–2,500 m water depth and includes the Antarctic Intermediate Water and North Atlantic Deep Water, and has long-term currents of ~4 cm s^{-1} with daily maximum velocities up to 35 cm s^{-1} (refs. 32,35). The entire water column may also be affected by the formation of mesoscale (>300 km diameter) southward-bound anti-cyclonic eddies due to the interaction between NEMC and Madagascar[30–32,36,37]. These eddies may alter the bottom current regime[12].

Bathymetry

Two separate multi-beam surveys covering the study site were collected in 2013 and 2014 with a Hugin 1,000 autonomous underwater vehicle using a Kongsberg EM2040 sonar with 140° swath width. Data were gridded into 5 m × 5 m bins and have a vertical resolution of approximately 0.1 m. A more focused (190-m-wide) bathymetric survey was also performed using a remotely operated vehicle, with data gridded to 0.6 m × 0.6 m bins, with a vertical resolution on the order of a few centimetres (Fig. 1e). Seabed data, including bathymetric elevation (Fig. 1a and Extended Data Fig. 2) and backscatter (that is, the strength of the signal reflected from the seabed, where dark colours represent more compact, consolidated, cemented and/or coarser-grained substrate; Fig. 1d) were provided in processed form by the energy company Eni, hence no processing of raw data was performed in this study. The bathymetric raster surface was used to generate a greyscale slope gradient attribute map in Environmental Systems Research Institute ArcGIS that was found to best illustrate the geomorphological features. These datasets were also analysed to determine the height of canyons and gullies. These heights were measured vertically from the deepest point of the canyon or gulley (that is, thalweg) to an inflection point on the flanking slope where the bathymetry levels out.

Moored instruments

Twelve moorings comprised paired single-point current metres that measured velocity and direction at 3 and 5 mAB (labelled C in Fig. 1). Two of these moorings (C05A and C05B) also held up-looking 300 kHz ADCPs positioned 10 mAB (accounting for blanking distance data collected from 15 mAB). The remaining 23 moorings included 600 kHz down-looking ADCPs that recorded vertical profiles either at 0.5 m resolution to within 10.5 m of the seabed (labelled CM in Fig. 1a) or at 1 m resolution to 11 mAB (labelled D in Fig. 1a). Data from two of the moorings (C02 and C08 located on open-slope areas; Fig. 1a) were previously reported in Fuhrmann et al.[15] ADCPs record current velocity (that is, speed and direction) and echo intensity at different elevations ('bins') within the water column. ADCP and current metre data were provided in text file format.

Near-bed current observations

The sense of near-bed flow at each mooring, and how it varies spatially across the study area, was assessed by extracting the velocity data from the bin closest to the seabed (Supplementary Table 1) and presented as rose diagrams that quantify both the speed and direction of near-bed currents (Fig. 1a). These current roses were overlain on the seabed bathymetric data to cross-compare the sense of direction with any geomorphological features (Fig. 1a). Time series analysis of near-bed currents at each mooring site were used to assess temporal variability (for example, Fig. 2a–d). Cumulative vector plots were then created to illustrate the net sense of near-bed flow and its evolution throughout the monitoring period (for example, Fig. 2d). To determine the extent to which topography influences the current regime, near-bed current velocity was extracted at different elevations above the seabed within a gulley, within a canyon and compared with that on an area of open slope, also presented as rose diagrams (Fig. 4).

Grain size measurements

Visual grain size (which typically discerns the 95th percentile)[55] core log observations were determined from box cores. To estimate surficial grain sizes a series of box core top observations were chosen to provide representative surficial grain sizes for different physiographic areas within the study site (Supplementary Table 3 and Fig. 1).

Estimates of sediment re-suspension

ADCP acoustic backscatter provides a proxy measure of suspended sediment concentration (for example, Fig. 2c,d and Extended Data Fig. 1). Backscatter is related to scattering of the acoustic pulses generated by the ADCP, which are enhanced by sediment suspensions, and records the strength of the returned signal. Higher echo intensities generally relate to higher suspended sediment concentrations until a concentration threshold is reached, at which point the signal will be fully attenuated[43]. Cross-comparison of near-bed currents obtained from instrument moorings and acoustic backscatter was used to investigate the influence of temporal variations in current speed and direction on sediment suspension (Fig. 2c,d and Extended Data Fig. 1).

To assess sediment mobility the critical Shields parameter[56] (θ_{cr}) was calculated for the range of grain sizes logged at the top of box cores for each of the physiographic settings within the study area. Sediment density values between 1,400 and 1,700 kg m^{-3} (as observed in gamma density analysis) were used to cover the range of sediment types/sizes. Near-bed current speeds from the medium to 95th percentile of representative moorings (Supplementary Table 3) were used as a range to calculate the Shields parameter[56] (θ) and determine whether near-bed currents were above the threshold for incipient motion (that is, where $\theta > \theta_{cr}$). Where the threshold for sediment mobility was exceeded, the Rouse number[57] (P) was calculated to define the mode of sediment transport as bedload ($P > 2.5$), suspension ($P < 1.2$), or a combination of both ($1.2 < P < 2.5$). Again, this calculation was based on the same range of grain sizes, densities and the subsequent settling velocities to provide a range in potential transport mechanisms. The Rouse number calculation assumed a natural grain shape of nominal size.

Modelled seawater velocity

Water column velocity models were analysed to link observed current velocity from moored instruments to mesoscales features (that is, eddies) and seasonal changes in ocean circulation (that is, the latitude NEMC diverges along the African margin; Fig. 1b). Data were acquired from the GLORYS12V1 global ocean eddy-resolving product hosted by

Copernicus Marine Data Store (https://data.marine.copernicus.eu) at 1/12° horizontal resolution. Modelled seawater velocity was analysed at the surface, ~500 m and ~1,700 m water depths, these water depths were chosen to correlate with the range of instrument mooring depths.

Data availability

ADCP and seafloor mooring data (used in Figs. 1 and 4 and Extended Data Fig. 1) can be requested through the 'System of Industry Metocean data for the Offshore and Research Communities' portal where they are held, http://www.simorc.com/welcome.asp. The GLORYS12V1 product (used to produce Fig. 3) from the EU Copernicus Marine Service Information is publicly available (https://doi.org/10.48670/moi-00021). The GEBCO 2022 Grid (https://www.gebco.net/data_and_products/historical_data_sets/#gebco_2022) was downloaded from the GEBCO portal (https://www.gebco.net/data_and_products/gridded_bathymetry_data/). Source data are provided with this paper.

References

51. Franke, D. et al. The offshore East African Rift system: structural framework at the toe of a juvenile rift. *Tectonics* **34**, 2086–2104 (2015).
52. Salman, G. & Abdula, I. Development of the Mozambique and Ruvuma sedimentary basins, offshore Mozambique. *Sediment. Geol.* **96**, 7–41 (1995).
53. Roberts, E. M. et al. Initiation of the western branch of the East African Rift coeval with the eastern branch. *Nat. Geosci.* **5**, 289–294 (2012).
54. Lutjeharms, J. R. E. Three decades of research on the greater Agulhas Current. *Ocean Sci.* **19**, 129–147 (2007).
55. Talling, P. J. On the frequency distribution of turbidite thickness. *Sedimentology* **48**, 1297–1329 (2001).
56. Soulsby, R. *Dynamics of Marine Sands* (Thomas Telford, 1997).
57. Rouse, H. Modern conceptions of the mechanics of fluid turbulence. *Trans. Am. Soc. Civ. Eng.* **102**, 463–505 (1937).

Acknowledgements

L.P.B. was supported by the Natural Environmental Council as part of the SPITFIRE doctoral training programme (Natural Environment Research Council grant no. NE/L002531/1). We thank Eni Rovuma Basin and Eni Mozambique for their approval of this study. M.A.C. recognizes funding from the UK Natural Environment Research Council Climate Linked Atlantic Sector Science project (NE/R015953/1). We thank the many individuals from the offshore teams of Fugro who enabled the acquisition of the seabed and ADCP data analysed.

Author contributions

The study design was conceived by M.A.C., I.A.K., L.P.B., R.A., G.M. and R.W. The field data acquisition was designed by M.F., R.A., G.M. and R.W. L.P.B. conducted the analysis with support from M.A.C. and J.E.H. L.P.B. prepared the figures and wrote the initial manuscript with contributions from M.A.C., I.A.K., E.M. and M.F. All authors contributed to editing the manuscript.

Competing interests

The authors declare no competing interests.

Additional information

Extended data is available for this paper at https://doi.org/10.1038/s41561-024-01494-2.

Supplementary information The online version contains supplementary material available at https://doi.org/10.1038/s41561-024-01494-2.

Correspondence and requests for materials should be addressed to Lewis P. Bailey.

Peer review information *Nature Geoscience* thanks David Mosher, Yulong Zhao and the other, anonymous, reviewer(s) for their contribution to the peer review of this work. Primary Handling Editor: Thomas Richardson, in collaboration with the *Nature Geoscience* team.

https://doi.org/10.1038/s41561-024-01494-2

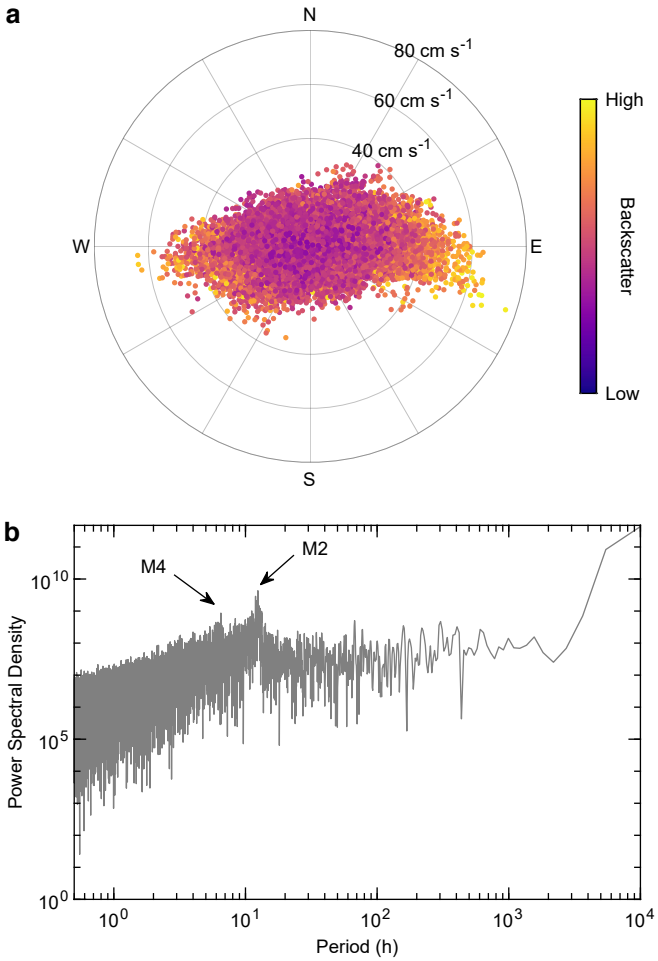

Extended Data Fig. 1 | Evidence for tidal signal and sediment re-suspension within Tungue Canyon at mooring C05A. a, Rose diagram showing the speed and direction for each measurement from the current metre located 3 mAB with data points coloured the corresponding ADCP acoustic backscatter measurement recorded at 15 mAB (that is the most bed proximal measurement). **b**, Power spectral density based on current direction measurements to show M2, semi-diurnal (12.4 h), and M4 (6.2 h) tidal constituents.

https://doi.org/10.1038/s41561-024-01494-2

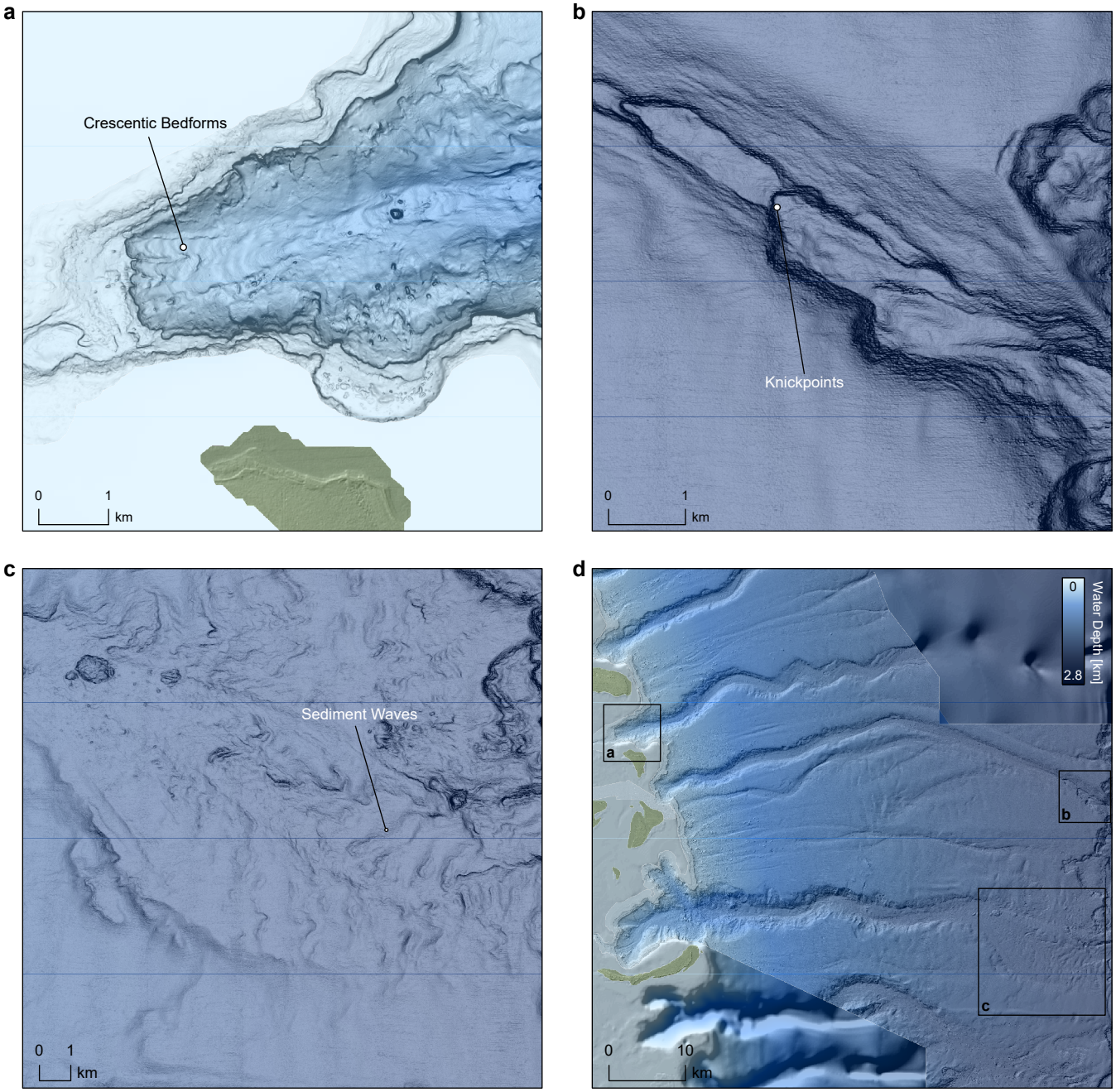

Extended Data Fig. 2 | Morphological evidence of past turbidity current activity. a, Crescentic bedforms in the head of Afungi Canyon. **b**, Knickpoints in the deep water section of Afungi Canyon. **c**, Sediment wave trains and large scale scours in Vamizi Canyon. **d**, Map of study area showing locations of morphological features.